An Integro-Differential Equation Formulation for the Ideal Veselago Lens

An Integro-Differential Equation Formulation for the Ideal Veselago Lens

Marzieh Eini Keleshteri* *(Member, IEEE)*, Martina Teresa Bevacqua† *(Member, IEEE)*, Vladimir Okhmatovski* *(Senior Member, IEEE)*, Tommaso Isernia† *(Fellow Member, IEEE)*, and Joe LoVetri* *(Senior Member, IEEE)*

***Abstract*—The 2D problem of finding the electric field for a line-source illuminating a lossless Veselago lens is cast as an integro-differential equation. The integral corresponds to a surface integral of the total tangential magnetic field on the boundaries of the lens. The integro-differential equation is obtained using an incident/scattered-field decomposition such that the Veselago lens is considered to be the scatterer. The new formulation is applied in five distinct regions: the illuminating-source region on the left side of the lens, two regions within the lens separated by a power-transfer plane, and two regions to the right of the lens, also separated by a power-transfer plane. The formulation is shown to be consistent with previously derived analytic expressions for the fields. In addition, the new integro-differential equation formulation provides a physically intuitive picture of the focusing behaviour of the lens, specifically, showing how the induced contrast sources at the boundaries determine the resulting focused field. It is shown how the line integral contributions to the scattered field on the left side of the lens is zero, and how the scattered field produces the expected focus point singularities on the interior and far-side of the lens.**

Keywords: Double-negative materials, inhomogeneous background, inverse scattering problem, Veselago lens

I. INTRODUCTION

A Veselago Lens (VL) is defined as a semi-infinite slab of double-negative material, *i.e.*, simultaneously having negative permittivity ($\epsilon_r = -1$) and permeability ($\mu_r = -1$) with no loss [1]. Predicted by Victor Veselago in 1968, the VL has since sparked significant interest in different fields, especially because of its potential to act as a perfectly focusing lens that creates two focus points, one inside and one outside of the lens, as shown in FIGURE 1. An approximation to this phenomenon, for the non-ideal case, was successfully demonstrated by Pendry in the lab. Working with a spectral domain analysis, it was shown that the ideal lens produces no reflection on the illuminating side where the source exists and the complete spectrum is transmitted and mirrored to the other side without suffering any distortion, [2].

This is the post-print version of the following article: M. Eini Keleshteri, Martina T. Bevacqua, V. Okhmatovski, T. Isernia and J. LoVetri, "An Integro-Differential Equation Formulation for the Ideal Veselago Lens," in IEEE Transactions on Antennas and Propagation, vol. 72, no. 6, pp. 5242-5251, June 2024, doi: 10.1109/TAP.2024.3400397. Article has been published in final form at: https://ieeexplore.ieee.org/document/10535051. 1558-2221

Marzieh Eini Keleshteri and Martina T. Bevacqua are both co-first authors.

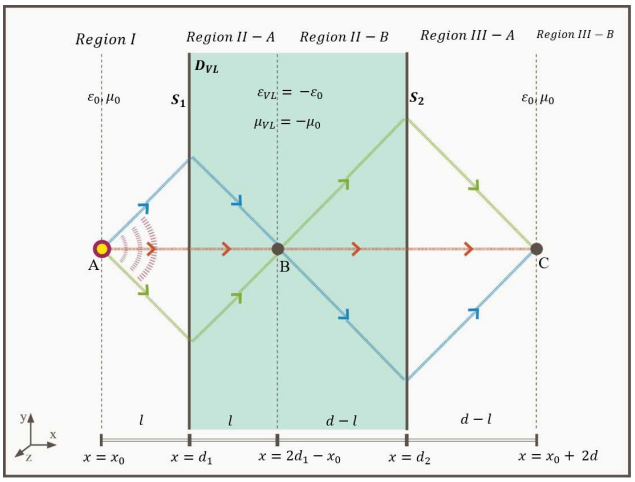

Fig. 1: A Veselago lens with thickness d by negative refraction focuses the waves emanating from a point source located at point A into two focus points B and C. The lens boundaries split the space into three main regions I, II and III, with two subdivisions II-A, II-B and III-A, and III-B in the second and third regions, before and after the focus singularities, [3], [4].

Several theoretical and numerical studies have been reported during the past two decades and many speculations on interpreting the physical viability of such a lens have been published, [5]–[9]. Moreover, the theoretical importance of the VL has been discussed in [4], [10], wherein it is shown that, if the VL could be actually implemented, it would lead to exceptional quantitative electromagnetic imaging. Subsequently, in [4], [11], the authors propose a numerical virtualization of the VL. Thus, having the true analytic expressions for the VL GF is indeed important. A comprehensive electromagnetic field analysis for both the 2D line-source and 3D vectorial point-source problems, including the case of such sources embedded in planar multi-layered media wherein any layer can have a positive or negative relative permittivity and permeability has been provided by Kong in [12].

In [12], Kong leaves all his expressions in terms of spectral-domain representations (see, *e.g.*, equations 190-209 of his paper) and provides limited comment on the convergence/divergence of these integrals. For the 2D slab, he concludes that the ideal VL acts to transfer the singularity of the point source to the other side of the VL: *It is seen that*

in the transmitted region, the field originates from a linear antenna located at $x = 2(d_2 - d_1)$, *which is a perfect image of the original antenna.* (Note that Kong assumes $x_0 = 0$.)

Within the VL Kong splits his solution over two regions: $d_1 < x < 2d_1$ and $2d_1 < x < d_2$. In the first region, Kong interprets his spectral-domain expression as a Hankel function, resulting in a singularity at the location $x = 2d_1$, but in the latter region, his spectral-domain expression is clearly divergent. Many scholars have opted to sidestep the contentious issue of whether the ideal VL has a bounded solution, justifiably, because it has been shown that when loss is added to the double negative material of the VL, the solution is indeed bounded. Moreover, physical realizations of a VL inevitably introduce loss, [13].

The issue of whether the ideal VL has a bounded solution has remained open until we published our solution in [3] and later in [4]. In Kong's spectral-domain expressions (197) and (201), he consistently takes the positive square-root of the dispersion relation, $\sqrt{k_0^2 - k_y^2}$ over the whole interior of the VL. Those expressions are written with respect to the distance $x - 2d_1$, which changes its sign across $x = 2d_1$. This makes the expression convergent and, equal to $H_0^{(2)}$ in the region $d_1 < x < 2d_1$. In the second region, $2d_1 < x < d_2$, the expression is clearly divergent, but the electric field remains continuous across the $x = 2d_1$ plane.

Other researchers have simply accepted that the solution to the ideal VL does not exist. For example in Chew's paper [14], he states, when speaking of the ideal double-negative half-space: *In this case, the reflection coefficient is zero for the perfectly matched case, and the transmission coefficient is one. The evanescent wave, however, will grow with distance away from the interface giving rise to a nonphysical solution and to a divergent integral.* The acceptance of this interpretation finds its rationale in the concept that the double-negative material of the VL amplifies the evanescent waves. That is true if one considers an evanescent wave of fixed k_y and then tracks its magnitude as a function of position z. But *at any fixed position* in the second part of the interior of the VL, $2d_1 < z < d_2$, the integral that sums all of the evanescent waves will diverge.

In a recent study by Eini *et al.* [3], also available in [4], analytical expressions for the steady-state electromagnetic field associated with an ideal Veselago lens were derived in 2D and 3D. The field expressions were obtained by considering power flow considerations and the imposition of appropriate boundary conditions (BCs) for both the 2D case of a line-source and the 3D case of an electric dipole point-source. The technique taken to derive the analytic field description in [3] was based on patching the solutions of the internal PDEs within the three main regions I-III shown in FIGURE 1 and matching the associated BCs along the boundaries of the VL. Moreover, the results verify the predicted focusing behaviour of the VL and amplification of the evanescent waves along the second boundary of the VL.

When represented in terms of Kong's spectral domain expressions, the solution in [3] is equivalent to switching the sign of the square root in the dispersion relation (or taking the (positive) distance from the internal singular point. These sacrifice the continuity of the electric field across $z = 2d_1$producing a complex-conjugate jump across the $z = 2d_1$ power transfer plane.

In this research, we formulate the electromagnetic field of a line-source in front of an ideal VL in terms of an integro-differential equation (IDE). The derivation is based on treating the VL as a scatterer and decomposing the VL total-field problem into an incident field due to the line-source radiating in free-space and a unique scattered field problem. This scattered-field problem contains two surface integrals (line integrals in the 2D case) that are due to the contrast created by the boundaries of the lens.

All three problems are formulated using the second-order Helmholtz equation, but the first-order Maxwell equations are used to obtain the inhomogeneous BCs at the VL boundaries. These are converted to surface distributions as inhomogeneous terms in the Helmholtz equation for the scattered field. The second-order equation is then inverted using Green's function (GF) of free space. The resulting IDE clearly shows the contribution of the inhomogeneous terms.

The IDE not only validates the novel expressions derived in earlier work, [3], but it provides fresh insights showing that the contrast sources are actually introduced only by the lens's boundaries. Moreover, the IDE formulation paves a path to dealing with an ideal double-negative lens of finite extent (*e.g*, a VL that is truncated), or of any shape. Thus, this methodology gives, in our view, an added value to the considerations expressed in [3].

The structure of this paper is outlined as follows. In Section II, a VL is defined, and its permittivity and permeability are introduced using a step-function approach. Subsequently, the total field problem is presented, and by employing the first-order Maxwell's equations, the total field is formulated as a PDE along with the corresponding BCs. The solution to this boundary value problem (BVP) is also introduced in this section.

Section II-A, by decomposing the total field into the incident field and scattered field in free space, the Helmholtz equation for the scattered field is derived. The relevant first-order Maxwell's equations for each subproblem are also presented in Appendix A.

Section II-B utilizes the derived Helmholtz equation to establish an IDE for the total field within the VL. The scattered field is expressed as a surface integral involving two improper integrals along the boundaries of the VL.

In Section III, we insert the analytic field expressions from [3], also presented in [4], into the IDE and show that they are consistent with the new mathematical formulation of the problem. Finally, the research concludes with Section IV, providing a summary of the findings and their implications.

II. Formulation of VL with 2D Excitation

We consider the VL to be an infinite slab of permittivity $\epsilon = -\epsilon_0$ and permeability $\mu = -\mu_0$ situated in free space and located between the surfaces $x = d_1$ and $x = d_2$. The width is denoted by $d = d_2 - d_1$. The surfaces of the VL will be denoted as

$$S_{VL} = S_1 \cup S_2, \tag{1a}$$

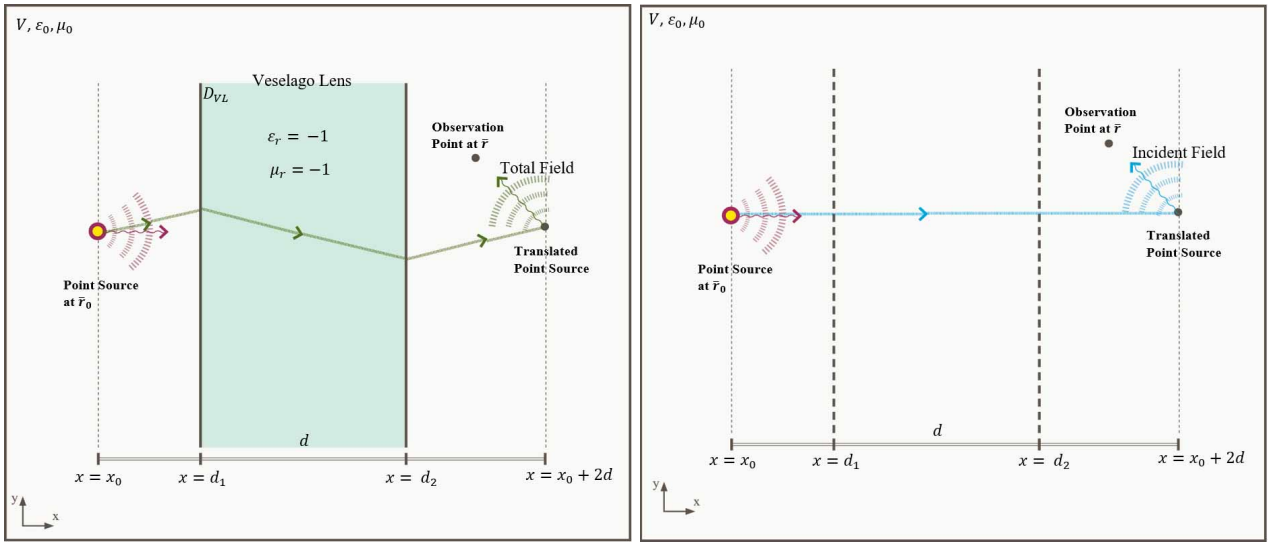

(a) Total-Field Problem

(b) Incident-Field Problem

Fig. 2: Fields associated with a point source in the presence of a VL slab. a) The total field is due to a point source located at a horizontal distance of at most d from the VL. b) The incident field is defined as that in free space with no lens.

where S_i is defined by

$$S_i \ = \{\bar{r} \in \mathbb{R}^2 |\ \bar{r} = (d_i, y)\}, \tag{1b}$$

for $i = 1, 2$. The domain of the VL is denoted as D_{VL} as shown in FIGURE 1. As we will only consider z-directed line-source excitations we can limit ourselves to the 2D xy-plane for the description of the geometry and the fields associated with such a source. Thus, we have a 2D TMz time-harmonic problem with $e^{j\omega t}$ time dependence, where $j^2 = -1$ and the radial frequency, ω, is fixed. The exponential time-dependence is henceforth dropped from the notation.

To easily manipulate the physical parameters of the VL we introduce the VL step-function

$$u_{s_{VL}}(x, y) \triangleq 1 - 2u_s(x - d_1) \ + \ 2u_s(x - d_2), \tag{2}$$

where

$$u_s(\xi) \ = \ \begin{cases} 0 & \xi < 0, \\ 1 & \xi > 0, \end{cases} \tag{3}$$

so that the permittivity and permeability functions become

$$\epsilon_{VL}(\bar{r}) \ \triangleq \ \epsilon_0 u_{s_{VL}}, \quad \text{and} \quad \mu_{VL}(\bar{r}) \ \triangleq \ \mu_0 u_{s_{VL}}, \tag{4}$$

respectively, for any position $\bar{r} = (x, y)$ in any of the three regions $x < d_1$, $d_1 \leq x \leq d_2$, and $x > d_2$, created by the VL and identified as I, II, and III and, respectively, in FIGURE 1.

A schematic of the total-field problem is shown in FIGURE 2a. We assume that a z-directed line-source of magnitude I is located on the left side of the VL at $\bar{r}_0 = (x_0, y_0)$ that can be described as the current density

$$\bar{J}(\bar{r}, \bar{r}_0) = I\delta(\bar{r} - \bar{r}_0)\ \hat{a}_z, \tag{5}$$

where $\hat{a}_z$ is the unit vector in the z-direction and $\delta(\cdot)$ is the Dirac delta function.

The 2D TMz electromagnetic field generated by the line source can be represented by the electric field component E_z, and magnetic field components H_x and H_y. All are bounded functions everywhere in $V \backslash \{\bar{r}_0\}$, including the VL boundaries. The tangential components are continuous across the boundaries, whereas the normal component of the magnetic field will suffer a jump across the VL boundaries. The field components are governed by the first-order Maxwell equations

$$j\omega\epsilon_{VL}(\bar{r})E_z - \partial_x H_y + \partial_y H_x \ = \ -I\delta(\bar{r} - \bar{r}_0), \tag{6a}$$

$$j\omega\mu_{VL}(\bar{r})H_x + \partial_y E_z \ = \ 0, \tag{6b}$$

$$j\omega\mu_{VL}(\bar{r})H_y - \partial_x E_z \ = \ 0, \tag{6c}$$

where ϵ_{VL} and μ_{VL} are defined as in (4).

Note that at the VL boundaries homogeneous BCs can be written for the electric field component:

$$\begin{cases} E_z(\bar{r}_S)^+ \ - \ E_z(\bar{r}_S)^- \ = \ 0, \\ \partial_x E_z(\bar{r}_S)^+ + \partial_x E_z(\bar{r}_S)^- \ = \ 0, \end{cases} \tag{6d}$$

where the superscripts $^-$ and $^+$, respectively, indicate the fields on the left and right sides of the surfaces S_i for $i = 1, 2$ and $\bar{r}_S \in S_1$ or S_2. The solution to this total-field interior BVP is the GF for the VL, which, converting to the notation used

herein, was given in [3] as

$$E_z(\bar{r}|\bar{r}_0, d_1, d) = -\frac{\omega\ \mu_0 I}{4}\begin{cases} H_0^{(2)}(k_0 R_0), & x \le d_1 \\ H_0^{(2)}(k_0 R_1), & d_1 \le x < 2d_1 - x_0 \\ H_0^{(1)}(k_0 R_1), & 2d_1 - x_0 < x \le d_2 \\ H_0^{(1)}(k_0 R_2), & d_2 \le x < x_0 + 2d \\ H_0^{(2)}(k_0 R_2), & x > x_0 + 2d, \end{cases} \quad (7)$$

where $R_0 = \|\bar{r} - \bar{r}_0\|$, $R_1 = \|\bar{r} - \bar{r}_1\|$, $R_2 = \|\bar{r} - \bar{r}_2\|$, $\bar{r}_1 = (2d_1 - x_0, y_0)$, and $\bar{r}_2 = (x_0 + 2d, y_0)$. We now derive an integral equation formulation for obtaining this GF.

A. Helmholtz Equation for the VL Scattered Field

Utilizing the equations for the total and incident field provided in Appendix A, we obtain a second-order PDE for the scattered field. Solving equations (60b) and (60c) respectively for H_x^s and H_y^s we find

$$H_x^s = \frac{-1}{j\omega\mu_0}\Big(\partial_y E_z^s + \chi_\mu H_x\Big), \quad (8a)$$

$$H_y^s = \frac{1}{j\omega\mu_0}\Big(\partial_x E_z^s - \chi_\mu H_y\Big). \quad (8b)$$

Then, substitute (8a) and (8b) into (60a), and multiply both sides of the obtained equation by the factor $j\omega\mu_0$ to get

$$-k_0^2 E_z^s - \partial_x\Big(\partial_x E_z^s - \chi_\mu H_y\Big) - \partial_y\Big(\partial_y E_z^s + \chi_\mu H_x\Big) = -j\omega\mu_0\chi_\epsilon E_z. \quad (9)$$

This is equivalent to

$$-k_0^2 E_z^s - \nabla^2 E_z^s + \partial_x(\chi_\mu H_y) - \partial_y(\chi_\mu H_x) = -j\omega\mu_0\chi_\epsilon E_z, \quad (10)$$

where $\nabla(\cdot)$ indicates the Laplacian operator. Note that taking derivatives of the step-function χ_μ as a piece-wise continuous function needs special attention. The derivative of this function with respect to variable y is zero as there is no discontinuity along the y-direction. Employing equation (1.62) on page 13 of [15] to χ_μ to find the distributional derivative of this function with respect to x we find

$$\begin{aligned}\partial_x\big(\chi_\mu(\bar{r})\big) &= \big[\chi_\mu(\bar{r}_{S_1})^+ - \chi_\mu(\bar{r}_{S_1})^-\big]\delta(x - d_1) \\ &+ \big[\chi_\mu(\bar{r}_{S_2}^+) - \chi_\mu(\bar{r}_{S_2})^-\big]\delta(x - d_2) \\ &= 2j\omega\mu_0\Big[\delta(x - d_2) - \delta(x - d_1)\Big]. \end{aligned} \quad (11)$$

Therefore, using (4), (10) can be revised as

$$\begin{aligned}&-k_0^2 E_z^s - \nabla^2 E_z^s + \chi_\mu\big[\partial_x H_y - \partial_y H_x\big] \\ &+ 2j\omega\mu_0\Big[\delta(x - d_2) - \delta(x - d_1)\Big]H_y \\ &= -j\omega\mu_0\chi_\epsilon E_z. \end{aligned} \quad (12)$$

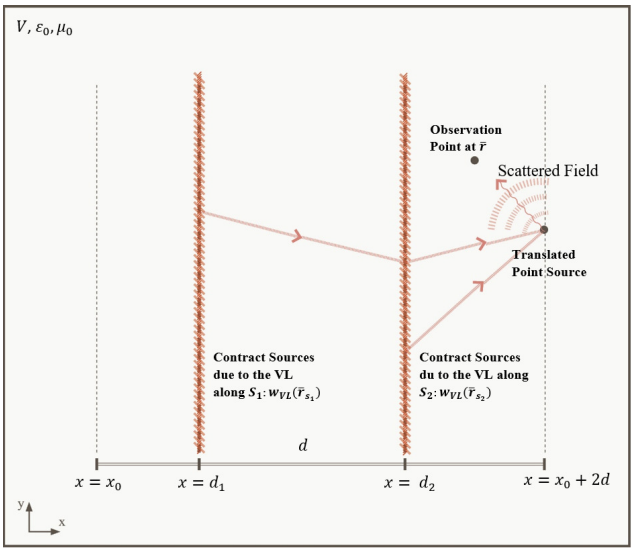

Fig. 3: A schematic of the scattered-field problem, obtained by subtracting the incident field from the total field shown in FIGUREs 2a and 2b. The contrast sources, w_{VL}, on the VL boundaries as the result of the presence of the VL in the total-field measurements.

Using (6a), the third expression on the left-hand side of (12) can be rewritten leading to

$$\begin{aligned}&-k_0^2 E_z^s - \nabla^2 E_z^s + \chi_\mu\big[j\omega\epsilon_{VL}(\bar{r})E_z + \delta(\bar{r} - \bar{r}_0)\big] \\ &+ 2j\omega\mu_0\Big[\delta(x - d_2) - \delta(x - d_1)\Big]H_y \\ &= -j\omega\mu_0\chi_\epsilon E_z. \end{aligned} \quad (13)$$

Finally, recalling the values of ϵ_{VL}, χ_ϵ, and χ_μ, respectively, in (4), (58), and (59) corresponding to the outside and inside the VL and noting that $\delta(\bar{r} - \bar{r}_0)$ is zero inside the VL, (13) can be simplified into the Helmholtz equation

$$\nabla^2 E_z^s + k_0^2 E_z^s = 2j\omega\mu_0\Big[\delta(x - d_2) - \delta(x - d_1)\Big]H_y. \quad (14)$$

This is the inhomogeneous scattered-field Helmholtz equation and the expression on the right-hand side (RHS) can be interpreted as the surface contrast sources created by the VL. This is symbolically shown in FIGURE 3 as $w_{VL}(\bar{r}_s)$. Note that volumetric contrast currents are not present and these surface contrast currents at the boundaries of the lens are solely responsible for the scattered field. The incident/scattered field decomposition allows us to discover the presence of these surface currents. This was not evident when the VL lens problem was solved by writing a Helmholtz equation in each of the three regions and enforcing the BCs at the VL boundaries as was done in [3].

B. Integro-differential Equation for Electric Field

Inverting the obtained Helmholtz equation in the previous section gives rise to an integral equation for the VL scattered

field as

$$E_z^s(\bar{r}) = \int_V G_0(\bar{r}|\bar{r}')\, 2j\omega\mu_0 \Big[\delta(x'-d_2) - \delta(x'-d_1)\Big] H_y(\bar{r}')\, dA', \tag{15}$$

where $G_0(\bar{r}|\bar{r}') = \frac{j}{4}H_0^{(2)}\big(k_0\|\bar{r}-\bar{r}'\|\big)$ is the free-space GF associated with solving (14) for any observation point $\bar{r} = (x, y)$, and $dA' = dx'dy'$. Substituting this into the above and employing the sifting property of the delta functions, this is written as two line integrals along the VL boundaries as

$$E_z^s(\bar{r}) = 2j\omega\mu_0 \Bigg\{ \int_{S_2} \frac{j}{4}H_0^{(2)}\big(k_0\|\bar{r}-(d_2,y')\|\big)\; H_y(d_2,y')\; dy' - \int_{S_1} \frac{j}{4}H_0^{(2)}\big(k_0\|\bar{r}-(d_1,y')\|\big)\; H_y(d_1,y')\; dy' \Bigg\}. \tag{16}$$

The total electric field of the VL can be formulated as

$$E_z(\bar{r}) = E_0^i(\bar{r}) + 2j\omega\mu_0 \int_{S_2} \frac{j}{4}H_0^{(2)}\big(k_0\|\bar{r}-(d_2,y')\|\big)\; H_y(d_2,y')\; dy' - 2j\omega\mu_0 \int_{S_1} \frac{j}{4}H_0^{(2)}\big(k_0\|\bar{r}-(d_1,y')\|\big)\; H_y(d_1,y')\; dy', \tag{17}$$

where $E_0^i(\bar{r})$ is the free-space incident field defined by relation (53).

Noting that H_y is related to E_z by (6c), this represents an IDE for the total field. It is best to leave H_y within the integral as it is continuous at the boundaries of the VL, whereas the normal derivative of the electric field is not continuous.

Solving this IDE provides an alternative method of obtaining the field of a line-source placed in front of a VL, and studying the scattering effects of the lens. Moreover, the IDE is propaedeutic to the calculation of the field for the case of an arbitrary scatterer in the presence of a VL. The field given in [3], and reproduced in (7), was obtained by patching together the continuous solutions within each of the five regions identified in FIGURE 1, and enforcing the relevant BCs at the VL boundaries. In addition, maintaining a causal direction of power flow in the field solutions within each region was used to determine the final form of the solution. Although solving this IDE provides an alternate means to getting the VL GF, it does not seem to be a simple task. On the other hand, this equation can be used as a means of verifying the solution given in (7).

III. Verification of the IDE

The analytic solution of this IDE requires specialized techniques that can be found in standard references, such as [16], [17]. The unknown fields can also be expanded using a spatial Fourier transform along S_1 and S_2.

On the other hand, approximate numerical techniques such as the Method of Moments can be used but the basis functions may have to be tailored to deal with the infinite extent of the domain.

Alternatively, we can verify the formulation of this IDE by showing that it is consistent with the analytic expressions for the VL Green's function derived in [3] and reproduced herein as (7). To do this, we simply plug-in the expressions for the electric and magnetic field obtainable from (7) into the IDE. Explicit expressions for the tangential total magnetic field can be found as

$$\mu_{VL} H_y(\bar{r}|\bar{r}_0) = \frac{1}{j\omega}\, \partial_x E_z(\bar{r}|\bar{r}_0). \tag{18}$$

These fields are required at the VL boundaries $x = d_1$ and $x = d_2$, but it should be noted that the VL permeability is defined using a step-function, μ_{VL}, that jumps at these locations, causing the discontinuity in the normal derivative of the electric field. On the other hand, the tangential magnetic field is continuous across the VL boundaries. Thus, by utilizing (18) with the solution (7) we can express the magnetic fields in the following manner at each boundary as

$$H_y(\bar{r}'|\bar{r}_0)\Big|_{x'=d_1} = \frac{C}{j\omega\mu_0}\, \frac{(x'-x_0)}{\|\bar{r}'-\bar{r}_0\|}\, H_1^{(2)}(k_0\|\bar{r}'-\bar{r}_0\|)\Big|_{x'=d_1} = \frac{C}{j\omega\mu_0}\, \frac{(d_1-x_0)}{\sqrt{(d_1-x_0)^2+(y'-y_0)^2}} \times H_1^{(2)}(k_0\sqrt{(d_1-x_0)^2+(y'-y_0)^2}), \tag{19}$$

and

$$H_y(\bar{r}'|\bar{r}_0)\Big|_{x'=d_2} = \frac{C}{j\omega\mu_0}\, \frac{(x'-x_0-2d)}{\|\bar{r}'-\bar{r}_2\|}\, H_1^{(1)}(k_0\|\bar{r}'-\bar{r}_2\|)\Big|_{x'=d_2} = \frac{C}{j\omega\mu_0}\, \frac{(d_2-x_0-2d)}{\sqrt{(d_2-x_0-2d)^2+(y'-y_0)^2}} \times H_1^{(1)}(k_0\sqrt{(d_2-x_0-2d)^2+(y'-y_0)^2}), \tag{20}$$

where $\bar{r}_2$ is as defined in (7) and the constant C is

$$C = \frac{k_0\omega\mu_0 I}{4}. \tag{21}$$

These can now be substituted into the expressions for the magnetic fields in the integrands of the first and second line integrals. Thus, we can express the equation (17) as

$$E_z(\bar{r}) = -\frac{\omega\mu_0 I}{4}H_0^{(2)}\big(k_0\|\bar{r}-\bar{r}_0\|\big) + I_S(\bar{r}), \tag{22}$$

where the line integral

$$I_S(\bar{r}) \triangleq I_{S_2}(\bar{r}) - I_{S_1}(\bar{r}), \tag{23}$$

consists of the two sub integrals

$$I_{S_1}(\bar{r}) \triangleq \frac{jC}{2}\int_{-\infty}^{\infty}\Bigg\{\frac{(d_1-x_0)}{\sqrt{(d_1-x_0)^2+(y'-y_0)^2}}\times H_0^{(2)}\big(k_0\sqrt{(x-d_1)^2+(y-y')^2}\big) \times H_1^{(2)}(k_0\sqrt{(d_1-x_0)^2+(y'-y_0)^2})\Bigg\}dy', \quad (24)$$

and

$$I_{S_2}(\bar{r}) \triangleq \frac{jC}{2}\int_{-\infty}^{\infty}\Bigg\{\frac{(d_2-x_0-2d)}{\sqrt{(d_2-x_0-2d)^2+(y'-y_0)^2}}\times H_0^{(2)}\big(k_0\sqrt{(x-d_2)^2+(y-y')^2}\big) \times H_1^{(1)}(k_0\sqrt{(d_2-x_0-2d)^2+(y'-y_0)^2})\big)\ dy'\Bigg\}. \quad (25)$$

Employing the analytic expressions for the VL electric field of (7) into the left-hand side of (22), finally, leads to the following five integral expressions corresponding to the five regions created by the VL

$$I_S(\bar{r}|\bar{r}_0,d_1,d) = I_{S_2}(\bar{r})-I_{S_1}(\bar{r}) = -\frac{\omega\mu_0 I}{4}\begin{cases}0, & x\le d_1,\\ H_0^{(2)}(k_0R_1)-H_0^{(2)}(k_0R_0), & d_1\le x<2d_1-x_0,\\ H_0^{(1)}(k_0R_1)-H_0^{(2)}(k_0R_0), & 2d_1-x_0<x\le d_2,\\ H_0^{(1)}(k_0R_2)-H_0^{(2)}(k_0R_0), & d_2\le x<x_0+2d,\\ H_0^{(2)}(k_0R_2)-H_0^{(2)}(k_0R_0), & x>x_0+2d.\end{cases} \quad (26)$$

These expressions represent the line integrals explicitly in terms of differences between translated Hankel functions and it is not at all obvious that these infinite line integrals should evaluate to such expressions in each region. Thus, in the next section, we provide an analytic verification that these infinite line integrals do indeed evaluate to the RHS of (26).

A. Analytic Verification of the Line Integrals

We proceed with revised expressions for the line integrals I_{S_1} and I_{S_2}, written in terms of the derivative of the electric field:

$$I_{S_1}(\bar{r}) = \frac{jC}{2}\int_{-\infty}^{\infty}\Big[H_0^{(2)}(k_0R')\,\frac{-1}{k_0}\frac{\partial}{\partial x'}H_0^{(2)}(k_0R_0')\Big]_{x'=d_1}dy', \quad (27)$$

and

$$I_{S_2}(\bar{r}) = \frac{jC}{2}\int_{-\infty}^{\infty}\Big[H_0^{(2)}(k_0R')\,\frac{-1}{k_0}\frac{\partial}{\partial x'}H_0^{(1)}(k_0R_2')\Big]_{x'=d_2}dy', \quad (28)$$

where $R'=\|\bar{r}-\bar{r}'\|$, $R_0'=\|\bar{r}'-\bar{r}_0\|$, $R_2'=\|\bar{r}'-\bar{r}_2\|$, and $\bar{r}_2=(x_0+2d,y_0)$ as previously defined.

Taking into account the observation that the partial derivative with respect to the parameter x' only differs by a minus sign compared to the partial derivative with respect to x_0 (if allowed to vary), we can rewrite equations (27) and (28) as follows

$$I_{S_1}(\bar{r}) = \frac{jC}{2k_0}\frac{\partial}{\partial x_0}\int_{-\infty}^{\infty}\Big[H_0^{(2)}(k_0R')\,H_0^{(2)}(k_0R_0')\Big]_{x'=d_1}dy', \quad (29)$$

and

$$I_{S_2}(\bar{r}) = \frac{jC}{2k_0}\frac{\partial}{\partial x_0}\int_{-\infty}^{\infty}\Big[H_0^{(2)}(k_0R')\,H_0^{(1)}(k_0R_2')\Big]_{x'=d_2}dy'. \quad (30)$$

Substituting $x'=d_1,d_2$ correspondingly into the integrands of (29) and (30), we find the equivalent expressions

$$I_{S_1}(\bar{r}) = \frac{jC}{2k_0} \quad (31)$$

$$\times\frac{\partial}{\partial x_0}\Bigg\{\int_{-\infty}^{\infty}H_0^{(2)}\big(k_0\sqrt{(x-d_1)^2+(y-y')^2}\big) H_0^{(2)}\big(k_0\sqrt{(d_1-x_0)^2+(y'-y_0)^2}\big)dy'\Bigg\}, \quad (32)$$

and

$$I_{S_2}(\bar{r}) = \frac{jC}{2k_0} \quad (33)$$

$$\times\frac{\partial}{\partial x_0}\Bigg\{\int_{-\infty}^{\infty}H_0^{(2)}\big(k_0\sqrt{(x-d_2)^2+(y-y')^2}\big) H_0^{(1)}\big(k_0\sqrt{(d_2-x_0-2d)^2+(y'-y_0)^2}\big)\ dy'\Bigg\}, \quad (34)$$

respectively.

Now, using the spectral domain definition of the Hankel Functions of zeroth order of the first and second kind, as presented in Appendix B, we can now rewrite the line integrals as

$$I_{S_1}(\bar{r}) = \frac{jC}{2\pi^2k_0}\frac{\partial}{\partial x_0}\int_{-\infty}^{\infty}dy'\Bigg\{\int_{-\infty}^{\infty}d\zeta_y\,\frac{e^{j\zeta_y(y-y')\ -\ j\zeta_x|x-d_1|}}{\zeta_x}\int_{-\infty}^{\infty}d\eta_y\,\frac{e^{j\eta_y(y'-y_0)\ -\ j\eta_x|d_1-x_0|}}{\eta_x}\Bigg\}, \quad (35)$$

and

$$I_{S_2}(\bar{r}) = \frac{jC}{2\pi^2k_0}\frac{\partial}{\partial x_0}\int_{-\infty}^{\infty}dy'\Bigg\{\int_{-\infty}^{\infty}d\zeta_y\,\frac{e^{j\zeta_y(y-y')\ -\ j\zeta_x|x-d_2|}}{\zeta_x}\int_{-\infty}^{\infty}d\eta_y\,\frac{e^{j\eta_y(y'-y_0)\ +\ j\eta_x|d_2-x_0-2d|}}{\eta_x}\Bigg\}, \quad (36)$$

where $\zeta_x = (k_0^2-\zeta_y^2)^{1/2}$ and $\eta_x = (k_0^2-\eta_y^2)^{1/2}$.

By rearranging the exponents, interchanging the integrals, and collecting the terms with the exponents depending on y'

into one integrand, we find

$$I_{S_1}(\bar{r}) = \frac{jC}{2\pi^2 k_0}\frac{\partial}{\partial x_0}\int_{-\infty}^{\infty} d\zeta_y \int_{-\infty}^{\infty} d\eta_y \frac{e^{j\zeta_y y - j\zeta_x|x-d_1|}}{\zeta_x}\frac{e^{-j\eta_y y_0 - j\eta_x|d_1-x_0|}}{\eta_x} \times \int_{-\infty}^{\infty} dy' e^{j(\eta_y-\zeta_y)y'}, \quad (37)$$

and

$$I_{S_2}(\bar{r}) = \frac{jC}{2\pi^2 k_0}\frac{\partial}{\partial x_0}\int_{-\infty}^{\infty} d\zeta_y \int_{-\infty}^{\infty} d\eta_y \frac{e^{j\zeta_y y - j\zeta_x|x-d_2|}}{\zeta_x} e^{-j\zeta_y y'}\frac{e^{-j\eta_y y_0 + j\eta_x|d_2-x_0-2d|}}{\eta_x} \times \int_{-\infty}^{\infty} dy' e^{j(\eta_y-\zeta_y)y'}. \quad (38)$$

Recalling the identity

$$\int_{-\infty}^{\infty} e^{j(\eta_y-\zeta_y)y'}\, dy' = 2\pi\delta(\eta_y-\zeta_y), \quad (39)$$

relations (37) and (38) are equivalent to

$$I_{S_1}(\bar{r}) = \frac{jC}{\pi k_0}\frac{\partial}{\partial x_0}\int_{-\infty}^{\infty} d\zeta_y \frac{e^{j\zeta_y y - j\zeta_x|x-d_1|}}{\zeta_x} \int_{-\infty}^{\infty} d\eta_y \frac{e^{-j\eta_y y_0 - j\eta_x|d_1-x_0|}}{\eta_x}\delta(\eta_y-\zeta_y), \quad (40)$$

and

$$I_{S_2}(\bar{r}) = \frac{jC}{\pi k_0}\frac{\partial}{\partial x_0}\int_{-\infty}^{\infty} d\zeta_y \frac{e^{j\zeta_y y - j\zeta_x|x-d_2|}}{\zeta_x} \int_{-\infty}^{\infty} d\eta_y \frac{e^{-j\eta_y y_0 + j\eta_x|d_2-x_0-2d|}}{\eta_x}\delta(\eta_y-\zeta_y), \quad (41)$$

respectively. Using the sifting property of the delta function, expressions (40) and (41) can be simplified into

$$I_{S_1}(\bar{r}) = \frac{jC}{\pi k_0} \times \frac{\partial}{\partial x_0}\int_{-\infty}^{\infty} d\zeta_y \frac{e^{j\zeta_y y - j\zeta_x|x-d_1|}}{\zeta_x}\frac{e^{-j\zeta_y y_0 - j\zeta_x|d_1-x_0|}}{\zeta_x}, \quad (42)$$

and

$$I_{S_2}(\bar{r}) = \frac{jC}{\pi k_0} \times\frac{\partial}{\partial x_0}\int_{-\infty}^{\infty} d\zeta_y \frac{e^{j\zeta_y y - j\zeta_x|x-d_2|}}{\zeta_x}\frac{e^{-j\zeta_y y_0 + j\zeta_x|d_2-x_0-2d|}}{\zeta_x}, \quad (43)$$

respectively. Multiplying the two fractions inside the integrands, these relations can be further simplified as

$$I_{S_1}(\bar{r}) \frac{jC}{\pi k_0} = \times\frac{\partial}{\partial x_0}\int_{-\infty}^{\infty} d\zeta_y \frac{e^{j\zeta_y(y-y_0) - j\zeta_x(|x-d_1|+|d_1-x_0|)}}{\zeta_x^2}, \quad (44)$$

and

$$I_{S_2}(\bar{r}) = \frac{jC}{\pi k_0} \times \frac{\partial}{\partial x_0}\int_{-\infty}^{\infty} d\zeta_y \frac{e^{j\zeta_y(y-y_0) + j\zeta_x(|d_2-x_0-2d|-|x-d_2|)}}{\zeta_x^2}, \quad (45)$$

respectively.

Observing FIGURE 1, it is evident that the point source in this problem is consistently positioned within Region I, while its image is consistently situated within Region III. Consequently, we always have the condition $x_0 < d_1$ and $d_2 < x_0 + 2d$. As a result, the exponent $|d_1 - x_0| = d_1 - x_0$, while the exponent $|d_2 - x_0 - 2d| = x_0 + 2d - d_2$. Therefore, we can conclude that

$$I_{S_1}(\bar{r}) = \frac{jC}{\pi k_0} \times \frac{\partial}{\partial x_0}\int_{-\infty}^{\infty} d\zeta_y \frac{e^{j\zeta_y(y-y_0) - j\zeta_x(|x-d_1|+(d_1-x_0))}}{\zeta_x^2}, \quad (46)$$

and

$$I_{S_2}(\bar{r}) = \frac{jC}{\pi k_0} \times \frac{\partial}{\partial x_0}\int_{-\infty}^{\infty} d\zeta_y \frac{e^{j\zeta_y(y-y_0) + j\zeta_x((x_0+2d-d_2)-|x-d_2|)}}{\zeta_x^2}. \quad (47)$$

Finally, taking the partial derivative with respect to x_0, we find

$$I_{S_1}(\bar{r}) = -\frac{C}{\pi k_0}\int_{-\infty}^{\infty} d\zeta_y \frac{e^{j\zeta_y(y-y_0) - j\zeta_x(|x-d_1|+(d_1-x_0))}}{\zeta_x}, \quad (48)$$

and

$$I_{S_2}(\bar{r}) = -\frac{C}{\pi k_0} \times \int_{-\infty}^{\infty} d\zeta_y \frac{e^{j\zeta_y(y-y_0) + j\zeta_x((x_0+2d-d_2)-|x-d_2|)}}{\zeta_x}. \quad (49)$$

To proceed, it is necessary to analyze the obtained integrals separately based on the sign of the exponents in the integrands and the location of the observation point in each of the five regions depicted in FIGURE 1, which are created by the VL. This approach allows for a comprehensive examination of the contributions from each region and ultimately enables us to derive the equivalent relations presented in the IDE (26). This is a key point with respect to the literature, for instance, [12].

To perform this analysis, we need to determine the sign of the expressions $|x-d_1|+(d_1-x_0)$ and $(x_0+2d-d_2)-|x-d_2|$ and identify the regions where these expressions are positive or negative. Subsequently, we can compare the obtained results with the definition of the Hankel Functions of zeroth order of the first and second kind, as outlined in equations (61) and (62) in Appendix B.

Let's begin by examining the exponent $|x - d_1| + (d_1 - x_0)$ in the line integral I_{S_1} and determining the conditions under which this exponent changes its sign. Noting that the illuminating point source is always located in the first region

in this problem, we observe that $d_1 > x_0$, and so $|x-d_1|+(d_1-x_0)$ is always positive. Comparing this result with the definition (62) in Appendix (B), we find that regardless of the observation point's position, the line integral always represents the Hankel function of the second kind.

However, when the observation point is located in Region I (i.e., $x < d_1$), we have $d_1 - x + d_1 - x_0 = 2d_1 - x - x_0$. Conversely, when the observation point is situated everywhere else i.e. $x > d_1$, we also have $x - d_1 + d_1 - x_0 = x - x_0$. Therefore, we can summarize the cases below

$$I_{S_1}(\bar{r}) \;=\; -\frac{\omega\mu_0 I}{4}\begin{cases} H_0^{(2)}(k_0R_1), & x < d_1, \\ H_0^{(2)}(k_0R_0), & x > d_1. \end{cases} \tag{50}$$

Let's now analyze the exponent $(x_0+2d-d_2)-|x-d_2|$ in the line integral I_{S_2} to determine the conditions under which this exponent changes its sign. Note that the exponent $(d_2 - x_0-2d)+|x-d_2|$ can take both positive and negative values. So, in the following, we will consider all the possible cases.

When $x-d_2>0$, the exponent $(x_0+2d-d_2)-(x-d_2) = (x_0+2d)-x$ is positive when $x < x_0+2d$. This situation occurs when the observation point is located in Region III-A. In this case, according to the definition (61) in Appendix (B), the line integral represents $\frac{\omega\mu_0 I}{4}H^{(1)}(k_0R_2)$.

On the other hand, when $x-d_2>0$, the exponent $(x_0+2d-d_2)-(x-d_2) = (x_0+2d)-x)$ is negative when we have $x > x_0+2d$, which corresponds to the observation point being situated in Region III-B. In this region, based on the definition (62) in Appendix (B), the line integral represents $\frac{\omega\mu_0 I}{4}H^{(2)}(k_0R_2)$.

Finally, when $x-d_2<0$, the exponent $(x_0+2d-d_2)-(d_2-x) = x+x_0-2d_1$ is negative when $x < 2d_1-x_0$. This case occurs when the observation point is located in Region I or II-A. In this case, according to the definition (62) in Appendix (B), the line integral represents $\frac{\omega\mu_0 I}{4}H^{(2)}(k_0R_1)$.

When the $x-d_2<0$, the exponent $(x_0+2d-d_2)-(d_2-x) = x+x_0-2d_1$ is positive when $x > 2d_1-x_0$. This case happens when the observation point is located in Region II-B. Therefore, according to the definition (61) in Appendix (B), the line integral represents $\frac{\omega\mu_0 I}{4}H^{(1)}(k_0R_1)$.

Therefore, the line integral I_{S_2} can be summarized into the following relation corresponding to the five different regions I to III-B:

$$I_{S_2}(\bar{r}) \;=\; -\frac{\omega\mu_0 I}{4}\begin{cases} H_0^{(2)}(k_0R_1), & x \le d_1, \\ H_0^{(2)}(k_0R_1), & d_1 \le x < 2d_1-x_0, \\ H_0^{(1)}(k_0R_1), & 2d_1-x_0 < x \le d_2, \\ H_0^{(1)}(k_0R_2), & d_2 \le x < x_0+2d, \\ H_0^{(2)}(k_0R_2), & x > x_0+2d. \end{cases} \tag{51}$$

Subtracting (50) correspondingly in the five regions from (51) gives rise to the required result of equation (26). This shows the consistency of the analytic expressions for the electromagnetic field of the VL obtained in [3] with the new IDE (26). Although not shown herein, the verification of these line integrals has also been performed using the asymptotic far-field expressions of the Hankel functions.

IV. Conclusion

An alternative methodology for describing the field of a line source in front of a VL that employs the decomposition of the total-field into an incident and scattered-field problem has been reported. This approach yields an IDE for the total field. The two line integrals of the total tangential magnetic field along the two boundaries of the VL represent the field scattered by the VL and capture the effect of the VL. Thus, the IDE offers valuable insights into the behavior of the lens, including scattering effects, focus point singularities, and the role of induced contrast sources at the boundary. This IDE has been utilized to validate the previously introduced five-region analytic form of the VL total field GF provided previously. Although not shown herein, the extension to a vectorial point-source excitation in front of a VL will yield an IDE involving surface integrals of the incident magnetic field over the planar boundaries of the VL. In addition to providing some insight into the functioning of the VL, the methodology utilized herein will be applicable to double-negative lenses of any shape, including a truncated VL slab. Indeed, any actual future realization of a VL will, of necessity, be a truncation of the slab. Then, the herein proposed approach is more general than the one in [3] and our contribution makes a first step towards such a more realistic situation. The technique is also easily extendable to the calculation of the electromagnetic field in case of an arbitrary scatterer in the presence of a VL. Furthermore, similar line-integral expressions occur when a virtual VL is introduced into the microwave imaging problem, [11].

Appendix A
Scattered/Incident Field Decomposition

A. Incident-Field Problem

The first step in obtaining the integral equation for the VL GF is to decompose the total field into the incident and scattered fields. As can be seen from FIGURE 2b, the incident field is defined as the field radiated by the line source in free space, that is, without the VL present. The boundary value problem (BVP) for the incident field is written as the PDEs

$$j\omega\epsilon_0 E^i_{0_z} - \partial_x H^i_{0_y} + \partial_y H^i_{0_x} \;=\; -I\delta(\bar{r}-\bar{r}_0), \tag{52a}$$

$$j\omega\mu_0 H^i_{0_x} + \partial_y E^i_{0_z} \;=\; 0, \tag{52b}$$

$$j\omega\mu_0 H^i_{0_y} - \partial_x E^i_{0_z} \;=\; 0, \tag{52c}$$

subject to the homogeneous BCs

$$\begin{cases} E^i_{0_z}(\bar{r}_S)^+ \;-\; E^i_{0_z}(\bar{r}_S)^- \;=\; 0, \\ \partial_x E^i_{0_z}(\bar{r}_S)^+ - \partial_x E^i_{0_z}(\bar{r}_S)^- \;=\; 0. \end{cases} \tag{52d}$$

Here the subscript is used to emphasize that this is the field in free-space, and the BCs along the surfaces S_1 and S_2 denoting the boundary where the VL would be if present, although not necessarily required, have been explicitly written because they

will be used in what follows. Taking the electric field as the primary unknown, the well-known solution to the above BVP for the electric field can be written in terms of free-space Green's function as

$$E^i_{0z}(\bar{r}) = -\frac{\omega\mu_0 I}{4}\, H^{(2)}_0(k_0\|\bar{r}-\bar{r}_0\|), \tag{53}$$

where k_0 is the free-space wavenumber and $H^{(2)}_0$ denotes the Hankel function of the second kind and zeroth order [18].

B. Scattered-Field Problem

For any field component, F, we can write the total field as a decomposition of the incident field plus a scattered field, as $F \triangleq F^i + F^s$. Therefore, subtracting the incident-field BVP from the total-field BVP we arrive at the BVP for the scattered field:

$$\begin{aligned} j\omega\epsilon_0 E^s_z - \partial_x H^s_y + \partial_y H^s_x &= -w_E, && \text{(54a)}\\ j\omega\mu_0 H^s_x + \partial_y E^s_z &= -w_{H_x}, && \text{(54b)}\\ j\omega\mu_0 H^s_y - \partial_x E^s_z &= -w_{H_y}, && \text{(54c)} \end{aligned}$$

where w_E, w_{H_x}, and w_{H_y} are contrast sources that have been introduced and must be determined such that the sum of the incident and scattered field BVPs equal that of the total field BVP.

To find the contrast sources w_E, w_{H_x}, and w_{H_y}, firstly add (52a - 52c) correspondingly to (54a - 54c) to obtain

$$\begin{aligned} j\omega\epsilon_0 E_z - \partial_x H_y + \partial_y H_x &= -I\delta(\bar{r}-\bar{r}_0) - w_E, && \text{(55a)}\\ j\omega\mu_0 H_x + \partial_y E_z &= -w_{H_x}, && \text{(55b)}\\ j\omega\mu_0 H_y - \partial_x E_z &= -w_{H_y}. && \text{(55c)} \end{aligned}$$

Then, subtract the obtained set of equations (55a - 55c) correspondingly from (6a - 6c) to find

$$\begin{aligned} j\omega(\epsilon_{VL}(\bar{r}) - \epsilon_0)E_z &= w_E, && \text{(56a)}\\ j\omega(\mu_{VL}(\bar{r}) - \mu_0)H_x &= w_{H_x}, && \text{(56b)}\\ j\omega(\mu_{VL}(\bar{r}) - \mu_0)H_y &= w_{H_y}. && \text{(56c)} \end{aligned}$$

We now define

$$w_E \triangleq \chi_\epsilon(\bar{r})E_z, \quad w_{H_x} \triangleq \chi_\mu(\bar{r})H_x, \quad w_{H_y} \triangleq \chi_\mu(\bar{r})H_y, \tag{57}$$

where χ_ϵ and χ_μ are the VL contrasts that can be defined in terms of ϵ_{VL} and μ_{VL} in (4) as

$$\chi_\epsilon(\bar{r}) \triangleq j\omega(\epsilon_{VL}(\bar{r}) - \epsilon_0) = \begin{cases} -2j\omega\epsilon_0 & \bar{r} \in D_{VL} \\ 0 & \bar{r} \notin D_{VL}, \end{cases} \tag{58}$$

and

$$\chi_\mu(\bar{r}) \triangleq j\omega(\mu_{VL}(\bar{r}) - \mu_0) = \begin{cases} -2j\omega\mu_0 & \bar{r} \in D_{VL} \\ 0 & \bar{r} \notin D_{VL}, \end{cases} \tag{59}$$

respectively. Note that these are discontinuous functions. Substituting (57) into the set of equations (54a) - (54c), gives rise to the PDEs

$$\begin{aligned} j\omega\epsilon_0 E^s_z - \partial_x H^s_y + \partial_y H^s_x &= -\chi_\epsilon(\bar{r})E_z, && \text{(60a)}\\ j\omega\mu_0 H^s_x + \partial_y E^s_z &= -\chi_\mu(\bar{r})H_x, && \text{(60b)}\\ j\omega\mu_0 H^s_y - \partial_x E^s_z &= -\chi_\mu(\bar{r})H_y. && \text{(60c)} \end{aligned}$$

Taking a similar approach, by subtracting the BCs (52d) from (6d), the BCs for the scattered field become

$$\begin{cases} E^s_z(\bar{r}_S)^+ - E^s_z(\bar{r}_S)^- = 0, \\ \partial_x E^s_z(\bar{r}_S)^+ + \partial_x E^s_z(\bar{r}_S)^- = -2\partial_x E^i_{0_z}(\bar{r}_S). \end{cases} \tag{60d}$$

APPENDIX B
THE INTEGRAL REPRESENTATION OF HANKEL FUNCTIONS OF ZEROth ORDER

Following [16], [19], [20], we arrive at the following expressions for $H^{(1)}_0$ and $H^{(2)}_0$, the Hankel function of zeroth order of the first and second kind

$$H^{(1)}_0(k\rho) = \frac{1}{\pi}\int_{-\infty}^{\infty} \frac{e^{jk_x x\, +\, jk_y|y|}}{k_y}\, dk_x, \tag{61}$$

and

$$H^{(2)}_0(k\rho) = \frac{1}{\pi}\int_{\infty}^{\infty} \frac{e^{-jk_x x\, -\, jk_y|y|}}{k_y}\, dk_x, \tag{62}$$

respectively, where according to the dispersion relation

$$k_y = (k^2 - k_x^2)^{1/2}. \tag{63}$$

In order for the integral (61) to be convergent, we have to ensure that

$$\Im\{k_y\} = \Im\{(k^2 - k_x^2)^{1/2}\} > 0, \tag{64}$$

where $\Im$ indicates the imaginary part of a complex number. Similarly, for the integral (62) to be convergent, we make sure that $\Im\{k_y\} = \Im\{(k^2 - k_x^2)^{1/2}\} < 0$.

REFERENCES

[1] V. G. Veselago, "The electrodynamics of substances with simultaneously negative values of ε and μ," *Physics-Uspekhi*, vol. 10, no. 4, pp. 509–514, 1968.

[2] J. B. Pendry, "Negative refraction makes a perfect lens," *Physical review letters*, vol. 85, no. 18, p. 3966, 2000.

[3] M. E. Keleshteri, V. I. Okhmatovski, and J. LoVetri, "Analytic sinusoidal steady-state electromagnetic field expressions for the ideal veselago lens," *IEEE Open Journal of Antennas and Propagation*, vol. 2, pp. 1057–1070, 2021.

[4] M. Eini Keleshteri, "A novel mathematical method for solving inverse scattering problems in microwave imaging using a virtual veselago lens," PhD thesis, University of Manitoba, August 2023, available at http://hdl.handle.net/1993/37491.

[5] S. A. Ramakrishna, J. Pendry, D. Schurig, D. Smith, and S. Schultz, "The asymmetric lossy near-perfect lens," *journal of modern optics*, vol. 49, no. 10, pp. 1747–1762, 2002.

[6] A. Lagarkov and V. Kissel, "Near-perfect imaging in a focusing system based on a left-handed-material plate," *Physical review letters*, vol. 92, no. 7, p. 077401, 2004.

[7] J. B. Pendry and D. R. Smith, "Reversing light with negative refraction," *Physics today*, vol. 57, pp. 37–43, 2004.

[8] J. Valentine, S. Zhang, T. Zentgraf, E. Ulin-Avila, D. A. Genov, G. Bartal, and X. Zhang, "Three-dimensional optical metamaterial with a negative refractive index," *nature*, vol. 455, no. 7211, pp. 376–379, 2008.

[9] R. E. Collin, "Frequency dispersion limits resolution in veselago lens," *Progress In Electromagnetics Research*, vol. 19, pp. 233–261, 2010.

[10] M. E. Keleshteri, V. Okhmatovski, I. Jeffrey, M. T. Bevacqua, T. Isernia, and J. LoVetri, "Demonstration of quantitative microwave imaging using an ideal veselago lens," *IEEE Open Journal of Antennas and Propagation*, pp. 1–1, 2022.
[11] M. E. Keleshteri, V. Okhmatovski, I. Jeffrey, M. T. Bevacqua, and J. LoVetri, "Assessing the potential of using a virtual veselago lens in quantitative microwave imaging," *Inverse Problems*, vol. 40, no. 3, p. 035001, 2024.
[12] J. A. Kong, "Electromagnetic wave interaction with stratified negative isotropic media," *Progress In Electromagnetics Research*, vol. 35, pp. 1–52, 2002.
[13] G. V. Eleftheriades and K. G. Balmain, *Negative-refraction metamaterials: fundamental principles and applications*. John Wiley & Sons, 2005.
[14] W. C. Chew, "Some reflections on double negative materials," *Progress In Electromagnetics Research*, vol. 51, pp. 1–26, 2005.
[15] J. Van Bladel and J. Van Bladel, *Singular electromagnetic fields and sources*. Clarendon Press Oxford, 1991.
[16] P. M. Morse and H. Feshbach, *Methods of theoretical physics*. New York: McGraw-Hill, Part I, 1953.
[17] C. Corduneanu, *Integral equations and applications*. Cambridge University Press Cambridge, 1991, vol. 148.
[18] R. F. Harrington, "Time-harmonic," *Electromagnetic Fields*, pp. 168–171, 2001.
[19] G. N. Watson, *A treatise on the theory of Bessel functions*. The University Press, 1922, vol. 3.
[20] W. C. Chew, Y. Wang, G. Otto, D. Lesselier, and J.-C. Bolomey, "On the inverse source method of solving inverse scattering problems," *Inverse Problems*, vol. 10, no. 3, p. 547, 1994.